

Can dark energy explain a high growth index?

Ícaro B. S. Cortês*

*Departamento de Engenharia de Computação e Automação,
Universidade Federal do Rio Grande do Norte, Caixa Postal 1524,
CEP 59078-970, Natal, Rio Grande do Norte, Brazil.*

Ronaldo C. Batista

*Escola de Ciências e Tecnologia, Universidade Federal do Rio Grande do Norte,
Caixa Postal 1524, CEP 59078-970, Natal, Rio Grande do Norte, Brazil.*

(Dated: September 10, 2025)

A promising way to test the physics of the accelerated expansion of the Universe is by studying the growth rate of matter fluctuations, which can be parametrized by the matter energy density parameter to the power γ , the so-called growth index. It is well-known that the Λ CDM cosmology predicts $\gamma = 0.55$. However, using observational data, Ref. [1] measured a much higher $\gamma = 0.633^{+0.025}_{-0.024}$, excluding the Λ CDM value within 3.7σ . In this work, we analyze whether Dark Energy (DE) with the Equation of State (EoS) parameter described by the CPL parametrization can significantly modify γ with respect to the predicted Λ CDM one. Besides the usual Smooth DE (SDE) scenario, where DE perturbations are neglected on small scales, we also consider the case of Clustering Dark Energy (CDE), which has more potential to impact the growth of matter perturbations. In order to minimally constrain the background evolution and assess the largest meaningful γ distribution, we use data from 32 Cosmic Chronometers, $H(z)$, data points. In this context, we found that both SDE and CDE models described by the CPL parametrization have almost negligible probability of providing $\gamma > 0.6$. However, given that the measured γ value assumes the Λ CDM background, a direct statistical measure of the incompatibility between theory and the measured value can not be done for other backgrounds. Thus, we devise a method in order to make a quick estimation of the γ constraints for CPL background. This method indicates that, when using DESI DR2 BAO data to constrain background parameters, no significant changes in the γ central value and uncertainty is observed. Consequently, both SDE and CDE described by CPL parametrization shall have a comparable level of tension with the expected γ measurements. Moreover, we present new fitting functions for γ , which are more accurate and general than the one proposed in Ref. [2] for SDE, and, for the first time, fitting functions for CDE models.

I. INTRODUCTION

The accelerated expansion of the Universe is still a big question in Cosmology. It can be explained either by a modified theory of gravity, or a unknown component of the universe, labeled as Dark Energy (DE) [3]. In the pursuit of more accurate data to answer this question, some tensions arose. The most significant one is known as the Hubble tension, which reflects the difference between measurements of the present expansion rate, H_0 , obtained locally by using the distance ladder methods [4] and globally, assuming the Λ CDM model, from Cosmic Microwave Background (CMB) data [5]. There is also the S_8 tension (where $S_8 \equiv \sigma_8 \sqrt{\Omega_{m0}/0.3}$, σ_8 is the amplitude of matter fluctuations at $8h^{-1}\text{Mpc}$ and Ω_{m0} is the matter density parameter now), which is related to the difference between the values of these parameters inferred from CMB [5] and measurements of galaxy clustering and weak gravitational lensing, as discussed in [6].

The S_8 tension is directly related to the growth of cosmic perturbations and has been analysed frequently in the literature, e.g., [7–9]. A particularly simple and

promising way to test how the physics of the accelerated expansion impacts the evolution of matter perturbations is by analyzing the growth rate of matter perturbations [10]

$$f = \frac{d \ln \delta_m}{d \ln a}, \quad (1)$$

which can be parametrized as [2]

$$f \simeq \Omega_m^\gamma, \quad (2)$$

where γ is a constant that depends weakly on the Equation of State (EoS) parameter of Smooth DE (SDE) models, $w(t) = p_{de}(t)/\rho_{de}(t)$, and $\Omega_m = \Omega_m(a)$ is the matter energy density parameter. For the Λ CDM cosmology, Refs. [2, 11] found $\gamma = 0.55$. However, using observational data, Ref. [1] found a much higher $\gamma = 0.633$ (implying a suppression of growth), excluding the Λ CDM value by 3.7σ , which can be referred as ‘ γ tension’. In the same work, it was also shown that a higher γ value reduces the S_8 tension from 3.2σ to 0.9σ .

This high value of γ naturally raises the question of what theoretical mechanisms are capable of producing it. In the case of SDE, it was shown that γ can be accurately described by the fitting function [2],

$$\gamma(w_1) = \begin{cases} 0.55 + 0.02(1 + w_1), & w_1 \leq -1 \\ 0.55 + 0.05(1 + w_1), & w_1 > -1 \end{cases}, \quad (3)$$

* icaro.cortes.710@ufrn.edu.br

where $w_1 = w(z = 1)$. This indicates that, for $w_1 \leq -1$, we would need $w_1 = 3.15$ to get $\gamma = 0.633$, in contradiction with the parametrization condition. For $w_1 > -1$, we would need $w_1 = 0.66$, which would generate a large DE density around $z = 1$. This simple extrapolation exercise indicates that it should be very difficult for SDE models to produce a high growth index. As we will show, with very loose constraints on the background evolution based on Cosmic Chronometers (CC) data, SDE with CPL parametrization has an almost negligible probability of producing $\gamma > 0.6$.

The usual assumption of SDE, in which one usually neglects DE perturbations on small scales, is based on Quintessence models [12–14]. In this case, DE is described by a minimally coupled canonical scalar field. The linear perturbations of this field propagate with sound speed $c_s = 1$, not allowing its perturbations to grow significantly on small scales. This approximation is well justified even in the nonlinear regime [15]. The simplest generalization of this scenario can be done by describing DE as a non-canonical minimally coupled scalar field, called k-essence [16, 17]. In this case, c_s can be chosen and DE perturbations can grow at small scales, see [18] for a more detailed discussion. In this work, we will consider the limiting case of $c_s \rightarrow 0$, in which DE perturbations have the maximal potential to grow and impact the evolution of matter perturbations. We refer to this scenario as Clustering DE (CDE), which growth index has already been studied in [19–22].

In this paper, we explore how SDE and CDE can change the growth index. We confirm the expectation based on the fitting formula (3) that SDE model can not provide $\gamma > 0.6$. We also find that CDE models can not raise the values of γ significantly.

As we will show, for the case of CDE, this result has a simple explanation. When $w(t) > -1$, DE perturbations have the tendency of being correlated with matter perturbations ($\delta_{de} \propto \delta_m$) and anti-correlated for $w(t) < -1$ ($\delta_{de} \propto -\delta_m$). In order to raise γ , DE perturbations must be anti-correlated with δ_m , causing a decrease in the gravitational potential and consequently slowing down the growth rate (higher γ). However, in the case $w(t) < -1$, the DE energy density decreases rapidly at high- z , thus the overall impact is very limited. On the other hand, the case $w(t) > -1$ can easily enhance the matter growth, thus providing significantly lower γ values, as already shown in [19].

Based on the samples of γ that we have computed using CC data, we were able to construct a new parametrization $\gamma = \gamma(w_1)$, which is more accurate than (3) and valid for larger parameter space. Moreover, for the first time, we present a γ parametrization for the case of CDE.

We also perform a more specific analysis using DESI DR2 Baryon Acoustic Oscillations (BAO) data, Ref. [23], plus CMB based priors to constrain background parameters. In this context, we make use of synthetic growth rate function to make a fast estimation of γ constraints beyond Λ CDM. This study suggests that the central val-

ues of γ and its uncertainty for w CDM and CPL models should be similar to the ones measured for Λ CDM.

The plan of this paper is as follows. In Sect. II, we define the background cosmology, the data, the parameters priors and statistics used to constrain the background evolution for the general analysis. In Sect. III, we present the equations for the evolution of matter and DE perturbations and discuss the accuracy of the constant- γ parametrization in describing $f(z)$. The resulting distributions for background parameters and γ and fitting functions are shown in Sect. IV. In Sect. V, we further constrain the background parameter using DESI BAO DR2 data and present a simple procedure to make a fast estimation of the γ constraints for models beyond Λ CDM and analyse the statistical compatibility between the theoretical values and the simulated measurements. We conclude in Sect. VI.

II. BACKGROUND COSMOLOGY

In this work, we assume General Relativity and a flat universe described by the Friedmann-Lemaître-Robertson-Walker metric, in which the line element is represented by

$$ds^2 = -c^2 dt^2 + a(t)^2 [dr^2 + r^2 d\Omega^2], \quad (4)$$

where $a(t)$ is the scale factor. As such, the square of the Hubble function can be written as

$$H^2 = \left(\frac{\dot{a}}{a}\right)^2 = H_0^2 (\Omega_{m0} a^{-3} + \Omega_{de}(a)), \quad (5)$$

where Ω_{m0} is the matter (dark matter plus baryons) density parameter now and $\Omega_{de}(a)$ is the DE energy parameter, which depends on the EoS assumed.

We consider that DE EoS is given by Chevallier-Polarski-Linder (CPL) [24, 25] parametrization:

$$w(a) = w_0 + w_a(1 - a). \quad (6)$$

Thus, the DE density parameter is given by

$$\Omega_{de}(a) = (1 - \Omega_{m0}) a^{-3(1+w_0+w_a)} \exp(-3w_a(1 - a)). \quad (7)$$

Besides the general case of free w_0 and w_a , we will also analyze the Λ limit ($w_0 = -1$ and $w_a = 0$) and constant EoS case (free $w \equiv w_0$ and $w_a = 0$). We refer to these models as CPL, Λ CDM and w CDM, respectively. In the general case, we have four free parameters: $h = H_0/(100\text{km s}^{-1}\text{Mpc}^{-1})$, Ω_{m0} , w_0 and w_a . Next, we discuss how to minimally constrain these parameters using $H(z)$ data.

Cosmic Chronometers Data

In order to minimally constrain the background evolution and the model parameters, we make use 32 of the

most recent CC data available, compiled by [26]. We use the Python library `Emcee` [27] as a Monte Carlo Markov Chain (MCMC) sampler and Python library `GetDist` [28] to analyse and plot the posteriors distributions.

There is a well-known discussion about the systematic errors in CC data, [29–31]. In these works, systematics of 15 of the 32 data points have been analyzed. Here, we split the dataset in two groups (with and without systematics), and χ^2 given by

$$\chi^2 = \chi_{\text{nosys}}^2 + \chi_{\text{sys}}^2, \quad (8)$$

where χ_{nosys}^2 is associated with the 17 data points without systematics, provided by [32–37], which reads

$$\chi_{\text{nosys}}^2 = \sum_i \left(\frac{\Delta H_i}{\sigma_i} \right)^2, \quad (9)$$

where $\Delta H_i = H_{\text{model}}(z_i) - H_{\text{data}}(z_i)$ and σ_i is the corresponding uncertainty of data points. The other part of the χ^2 associated with data points with systematics is given by

$$\chi_{\text{sys}}^2 = \Delta \vec{H}^T \mathbf{Cov}^{-1} \Delta \vec{H}, \quad (10)$$

where $\Delta \vec{H}$ is a vector with ΔH_i components associated with the 15 data points provided by Refs. [29–31], and \mathbf{Cov} is the corresponding covariance matrix for the BC3 model, available at <https://gitlab.com/mmoresco/CCcovariance>.

We sample the posterior distribution of the vector of parameters $\theta = (h, \Omega_{m0}, w_0, w_a)$, given by

$$\mathcal{L}(\theta|D) \propto P(\theta) L(D|\theta), \quad (11)$$

where

$$L(D|\theta) \propto \exp\left(-\frac{\chi^2}{2}\right) \quad (12)$$

is the likelihood of the data D given θ and $P(\theta)$ indicates the priors assumed for the parameters, listed in Tab. I. We also implement an additional flat prior to exclude cosmologies in which $\Omega_{de}(z=1000) > 0.01$, where $z = 1/a - 1$ is the redshift. This condition is similar to the assumption $w_0 + w_a < -0.1$ described by [38]. Allowing for DE models with non-negligible energy density at high- z , besides being highly disfavored by data [39], invalidates the Einstein-de-Sitter initial conditions used to solve the evolution of matter and DE perturbations, which will be discussed in detail in the next section.

We will discuss the MCMC results regarding the background parameters in the section IV, together with the results for γ .

III. GROWTH OF COSMOLOGICAL PERTURBATIONS

In a universe with SDE, the linear evolution of the matter density contrast, $\delta_m \equiv \rho_m/\bar{\rho}_m - 1$, is solely affected by the background expansion, as described by the

Table I. Priors for all parameters.

Parameter	Prior
h	$\mathcal{U}[0.5, 1]$
Ω_{m0}	$\mathcal{U}[0.01, 0.99]$
w	$\mathcal{U}[-3, -1/3]$
w_0	$\mathcal{U}[-3, 1]$
w_a	$\mathcal{U}[-3, 3]$

equation

$$\delta_m'' + \left(2 - \frac{1 + 3w(a)\Omega_{de}(a)}{2} \right) \frac{\delta_m'}{a} - \frac{3}{2} \frac{\Omega_m(a)}{a^2} \delta_m = 0, \quad (13)$$

where the prime denotes a derivative with respect to the scale factor. Starting the integration at a high redshift, $z_i = 1000$, initial values can be computed using the analytical solution for a matter-dominated Einstein-de-Sitter (EdS) universe $\delta_{mi}' = \delta_{mi}/a_i$, where we assumed $\delta_{mi} > 0$.

In the case of CDE, δ_m is also affected by DE perturbations, δ_{de} , whose effect is maximized for DE models with negligible sound speed. In this work, we consider the extreme case $c_s = 0$ based on the fluid description of DE and phenomenologically allowing for an EoS which can be non-phantom ($w(t) > -1$), phantom ($w(t) < -1$) or transit between these regimes. In this context, matter and DE perturbations obey the following system of equations [18]:

$$\begin{cases} \delta_m' + \frac{q}{a^2} & = 0, \\ \delta_{de}' - 3\frac{w}{a}\delta_{de} + (1+w)\frac{q}{a^2} & = 0, \\ q' - \frac{1}{2}(1+3w\Omega_{de})\frac{q}{a} + \frac{3}{2}(\Omega_m\delta_m + \Omega_{de}\delta_{de}) & = 0, \end{cases} \quad (14)$$

where $q \equiv \theta/H$ and $\theta = \vec{\nabla} \cdot \vec{v}$ is the divergence of the peculiar velocity of the DE-matter fluid. Note that the equation for the peculiar velocity is the same for matter and CDE because we are considering $c_s = 0$. To compute the initial conditions for DE perturbations, we use the solution valid for constant w in matter-dominated era [40–43]

$$\delta_{de} = \frac{1+w}{1-3w} \delta_m. \quad (15)$$

Although solution (15) only gives a general qualitative behavior at low- z [43], it can help us to predict the influence of CDE on the growth of δ_m . When $w(a) < -1$ we have the tendency $\delta_{de} \propto -\delta_m$, while for $w(a) > -1$ we have $\delta_{de} \propto \delta_m$. If the EoS is always phantom or non-phantom, these relations are always valid. In the case that the EoS transits between phantom and non-phantom or vice-versa, the actual relation between δ_{de} and δ_m might take some time to achieve the expected behavior. The general trend is clear: phantom EoS will induce negative δ_{de} , lowering the clustering power encoded in the last

term of Eq. (14), whereas non-phantom EoS enhances growth. Therefore, the desired higher values of γ could be obtained in phantom CDE models.

We solve Eqs. (13) and (14), then determine the growth rate $f = d \ln \delta_m / d \ln a$ and fit a constant γ assuming $f = \Omega_m^\gamma(a)$ for all the posterior distribution obtained. In this process, it is important to ask whether the fitted values of γ can accurately describe f . In the paper [2], where the fit (3) was introduced for the SDE model described by CPL parametrization, the accuracy of the fit was reported with respect to the growth variable $g \equiv \delta/a$. Accuracies better than 0.05% for Λ CDM with $\Omega_{m0} \in [0.22, 1]$ were reported, and 1% when lowering the limit to $\Omega_{m0} = 0.01$. For $w \neq -1$, the paper reported an accuracy within 0.4% for $w = -0.5$ and for dynamical EoS 0.25% when $w_0 = -0.82$ and $w_a = 0.58$. Here, we first will check how accurately a constant γ can reproduce f . In the next section, we will propose and analyze a new fitting function for γ .

In this work, we report the distribution of percent residuals given by the Root Mean Square (RMS) of $1 - \Omega_m^{\gamma_{\text{num}}}(z) / f_{\text{num}}(z)$, where f_{num} is the numerical solution and γ_{num} the corresponding fitted γ value. We compute the RMS percent residuals along 10 evenly spaced values of $0 \leq z \leq 2$, and show its distribution in Fig. 1 for all sets of parameters obtained in the MCMC analysis presented in Sect. IV. As can be seen, a very small fraction of models have residuals greater than 0.5%. The worst case occurs for CDE-CPL, reaching up to 4%, but still for a small fraction of the realizations. In general, all models present a concentration of residuals close to 0.15%. We also have checked that the largest residuals are mainly associated with low Ω_{m0} values. This demonstrates that, considering the CPL EoS, the constant γ parametrization for the growth rate is very reliable, even in the case of CDE. However, for more complex EoS parametrizations and for realizations including a non-negligible DE density at high- z , the constant- γ parametrization might not be adequate [19].

IV. GENERAL DISTRIBUTION OF γ

The parameter posteriors for Λ CDM, w CDM and CPL models are presented in figures 2, 3 and 4, respectively. Regarding the background parameters, we can see in Fig. 2 that CC data can constrain the two free parameters, Ω_{m0} and h , in the Λ CDM model. For w CDM this is not case, mainly because w is being limited by the prior assumed, but note that the posterior also shows some preference for $w \simeq -1$. Fig. 4 also shows that CPL parameters, w_0 and w_a , can not be constrained by CC data. The posteriors of w_0 and w_a are dominated by the flat priors shown in Tab. I together with the condition $\Omega_{de}(z = 1000) < 0.01$. The mean values for the marginalized 1D distributions are given in Tab. II. The number of samples in our chains is $N \sim 1000\tau$, where τ is the largest auto-correlation time of the parameters.

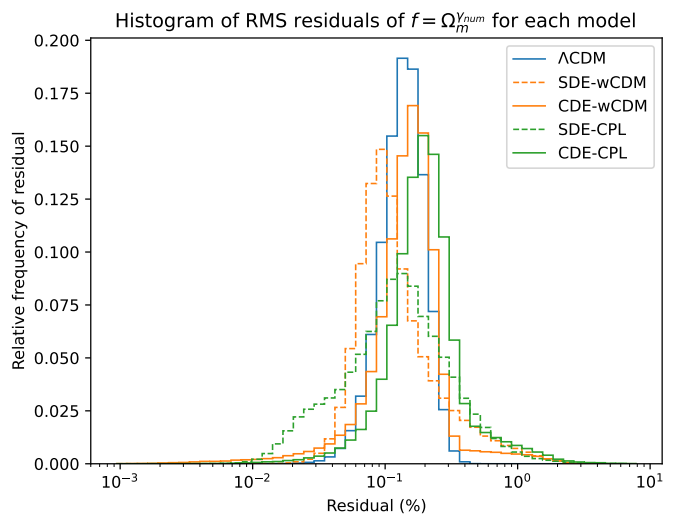


Figure 1. Histogram of RMS percent residuals for the constant growth index fit, with respect to the numerical solution of f for each model, normalized by relative frequency.

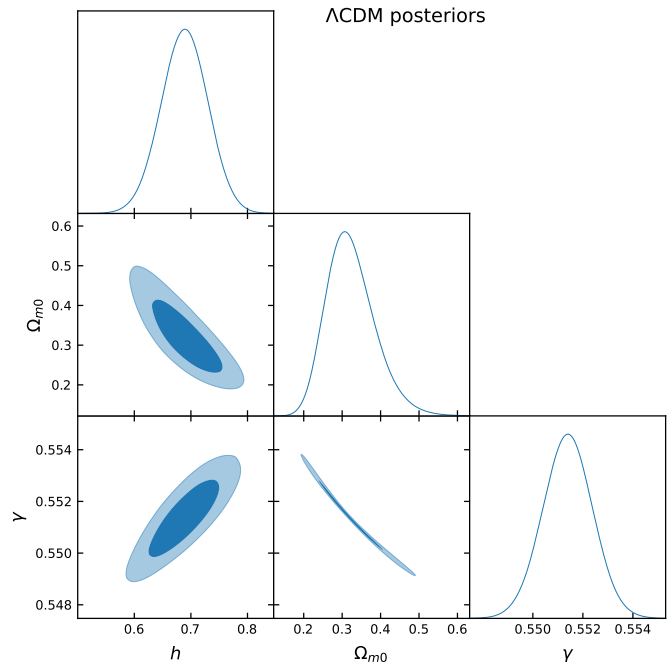


Figure 2. Marginalized posterior distributions for the Λ CDM background parameters, subjected to CC data and corresponding γ values given by integration of Eq. (13).

This is well beyond the suggested $N > 50\tau$ described in [27] as convergence criteria.

We recall that the main purpose of this analysis is to provide a wide, but still meaningful, distribution of background parameters that can be used to compute the linear growth of matter perturbations and γ . As can be seen in figures 2, 3 and 4, despite this large variation of the EoS parameters, γ can be determined with much smaller

variation.

The Λ CDM posteriors shown in Fig. 2 display a great determination of the growth index at $\gamma_\Lambda = 0.5514 \pm 0.0010$, agreeing with the previous results from Refs. [2, 11]. However, using data from Cosmological Microwave Background, galaxy surveys and Baryon Acoustic Oscillation (BAO) data, Ref. [1] found a value of $\gamma_m = 0.633^{+0.025}_{-0.024}$, excluding the Λ CDM value within 3.7σ , also showing that this value effectively solves the S_8 tension. Assuming normally distributed probabilities for the measured value and the Λ CDM one, with mean and standard deviation given in Tab. II, a simple quantification of the tension between these values is given by

$$\#\sigma = \frac{|\gamma_m - \gamma_\Lambda|}{\sqrt{\sigma_m^2 + \sigma_\Lambda^2}} = 3.26 \quad (16)$$

where we used $\sigma_m = 0.025$. If we assume the usual value $\gamma_\Lambda = 0.55$ and neglect its uncertainty, we get 3.32σ .

Now let us check whether more general SDE models and their CDE counterparts can provide high γ values. Although the analysis in Ref. [1] assumes the Λ CDM background to produce the γ constraints, assessing the possible values of γ in more general background and perturbative models will help us to identify scenarios in which γ can be increased and how likely this can happen. In the next section, we will address the statistical compatibility between theoretical values γ and its estimated value and uncertainties in models beyond Λ CDM.

We first analyze the correlations between the γ and the EoS parameters and how γ changes with respect to the Λ CDM value. The clearest case is for w CDM model, Fig. 3, but the following analysis also holds for CPL model. For $w > -1$ (non-phantom EoS) we have lower $\Omega_m(z)$ in the past with respect to the $w = -1$ case. In the SDE scenario, this behavior causes a suppression of growth, giving a higher γ . In the case of CDE, this correlation is inverted because $w > -1$ induces positive δ_{de} , which will act as an extra source of the gravitational potential, enhancing the growth and lowering γ . For $w < -1$ (phantom EoS) we have higher $\Omega_m(z)$ in the past with respect to $w = -1$. In SDE case, this induces a lower γ . Again, CDE inverts this correlation because now negative δ_{de} is induced, reducing the source of the gravitational potential, consequently increasing γ . These correlations also hold for CPL, but since many realizations shown in Fig. 4 include transitions from phantom to non-phantom EoS and vice-versa, they are not very clearly visualized. However, in terms of w_1 , these correlations become more evident in the upper panels of Fig. 7. Therefore, we can summarize the impact of DE model in the γ , with respect to the Λ CDM value, as follows:

- SDE, non-phantom EoS: $\gamma > 0.55$
- SDE, phantom EoS: $\gamma < 0.55$
- CDE, non-phantom EoS: $\gamma < 0.55$
- CDE, phantom EoS: $\gamma > 0.55$

It is also interesting to check the frequency of positive or negative occurrences of δ_{de} for the CDE scenario. In Fig. 5, we present the distribution of δ_{de}/δ_m at $z = 0$ and $z = 0.5$. We can see a small preference for negative δ_{de} , which is associated with the allowed values of the EoS parameters as follows. For non-phantom EoS, $\Omega_{de}(z)$ can be large at intermediate and high- z , a situation that is disfavored by data, e.g., [39]. In our analysis, this fact is mainly implemented with the prior $\Omega_{de}(z = 1000) < 0.01$. On the other hand, for phantom EoS, $\Omega_{de}(z)$ is very small at intermediate and high- z and can still induce an adequate accelerated expansion at low- z . Therefore, the allowed parameter space for the EoS parameters has a larger fraction of phantom realizations. As a consequence, given the correlations between w and δ_{de} explained earlier, we see some preference for $\delta_{de} < 0$.

In Fig. 6 we show a direct comparison between the γ distributions obtained. As can be seen, the SDE models are similar, regardless of the EoS parametrization. The same happens for the CDE models. Given the larger fraction of phantom realizations, SDE models have a slight preference for $\gamma < 0.55$, whereas CDE prefers $\gamma > 0.55$. The γ distributions for non- Λ models have greater variance and asymmetry. However, none of these models provide a significant fraction of realizations with $\gamma > 0.6$.

Note that, in Fig. 6, the γ distribution is heavy tailed for CDE models, then the reported mean value can lie outside the 1σ interval reported in Tab. II. We verified that the best fit model parameters lie within 1σ of the 1D marginalized distributions.

Table II. Marginalized 1D constraints and 68% C.L. intervals for the parameters of each cosmology subjected to CC data.

Parameter	Λ CDM	w CDM	CPL
h	0.689 ± 0.041	$0.727^{+0.054}_{-0.092}$	$0.733^{+0.069}_{-0.10}$
Ω_{m0}	$0.324^{+0.049}_{-0.072}$	0.296 ± 0.076	$0.319^{+0.060}_{-0.082}$
w or w_0	---	$-1.42^{+0.97}_{-0.37}$	$-1.47^{+0.91}_{-0.72}$
w_a	---	---	$-0.6^{+1.1}_{-2.0}$
γ (SDE)	0.5514 ± 0.0010	$0.5465^{+0.0054}_{-0.021}$	$0.5412^{+0.0056}_{-0.015}$
γ (CDE)	---	$0.545^{+0.019}_{-0.0061}$	$0.556^{+0.013}_{-0.00039}$

We could expect that phantom CDE models are able to produce high γ values because, as explained earlier, the associated negative δ_{de} operates in this direction. However, given that the gravitational potential depends on $\Omega_{de}\delta_{de}$ and, in the phantom case, Ω_{de} is small at intermediate and high- z , the actual impact of these models on γ is very limited. Consequently, although some preference for $\gamma > 0.55$ can be seen in Fig. 6, the highest possible values virtually never reach $\gamma \gtrsim 0.58$.

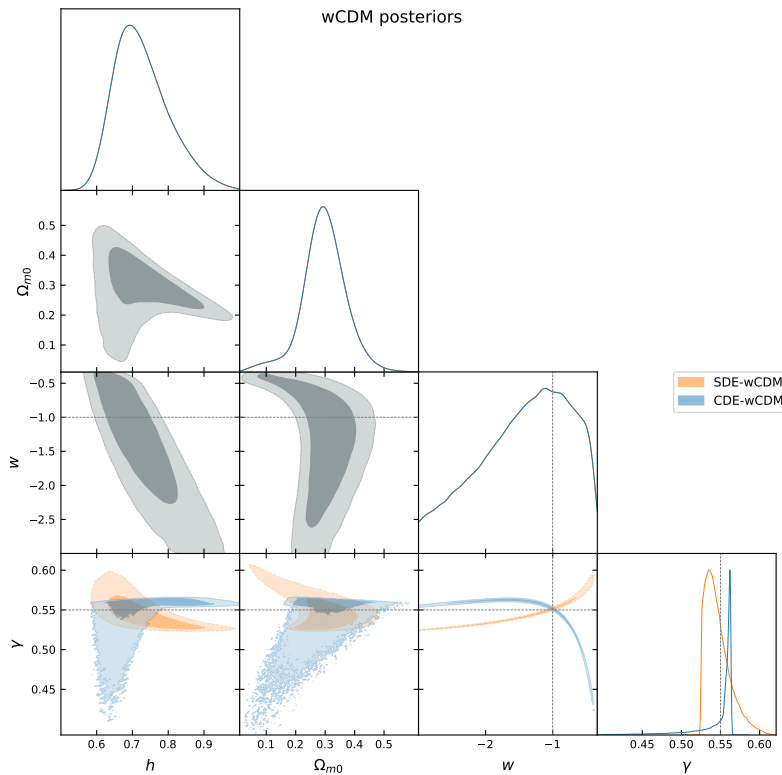


Figure 3. Marginalized posterior distributions for the w CDM models, with a shared background and distinct Smooth and Clustering Dark Energy growth index distributions. The dashed lines indicate the values of the Λ CDM parameters.

New fits for $\gamma(w)$

With the posterior distributions obtained, we were able to find a more accurate and general fitting function for γ , given by

$$\gamma(w_1) = aw_1 + be^{cw_1} + d, \quad (17)$$

The coefficients for each model are listed in Tab. III. The tested range of w_1 is $[-3, -1/3]$. The main difference between SDE and CDE models is the sign of the coefficient in the exponential term.

Table III. Coefficients for the fits of $\gamma(w_1) = aw_1 + be^{cw_1} + d$ for each model.

Model	Cosmology	a	b	c	d
SDE	w CDM	0.0101	0.1266	2.8013	0.5532
SDE	CPL	0.0068	0.1346	2.8453	0.5493
CDE	w CDM	0.0047	-0.6320	3.8570	0.5706
CDE	CPL	0.0045	-0.4673	3.2250	0.5738

The quality of the fits are demonstrated in the upper panels of Fig. 7, where our fits are well contained within the posteriors contours. The lower panels show the residuals of the parametrization of Eq. (3) and ours. We computed these residuals with the same RMS definition used for Fig. 1.

Let us first analyze the results for SDE in Fig. 7. Our fit is most accurate for the w CDM model (left panels), presenting a mode of residuals at 0.1%, while the linear fit of Eq. (3) presents a mode around 0.25%. In any case, very few realizations have residuals $> 1\%$. For the CPL models (right panels), our fit is noticeably better than the one of Eq. (3). For instance, the linear fit residuals, Eq. (3), peaks around 1% while the exponential fit, Eq. (17), peaks at 0.2%. The main reason for this improvement is that the linear fit does not perform well for $w_1 < -2$, as can be seen in the top panels of Fig. 7. We have tested whether there is some improvement in the fits quality when changing the pivot $w(z = 1)$ to other values. For $w(z = 1.2)$ and $w(z = 0.8)$, we noticed no relevant modifications in the histograms of residuals.

Our fitting function for γ can also be used to describe the values for the CDE case, which are shown with orange lines and contours in Fig. 1. As can be seen, it also performs very well in models with clustering DE. The modes of the RMS residuals is around 0.1% for both $w = \text{const.}$ and CPL parametrizations.

V. ESTIMATING THE γ TENSION BEYOND Λ CDM

So far, we have analyzed the distribution of γ based on the very loose constraints on background evolution given

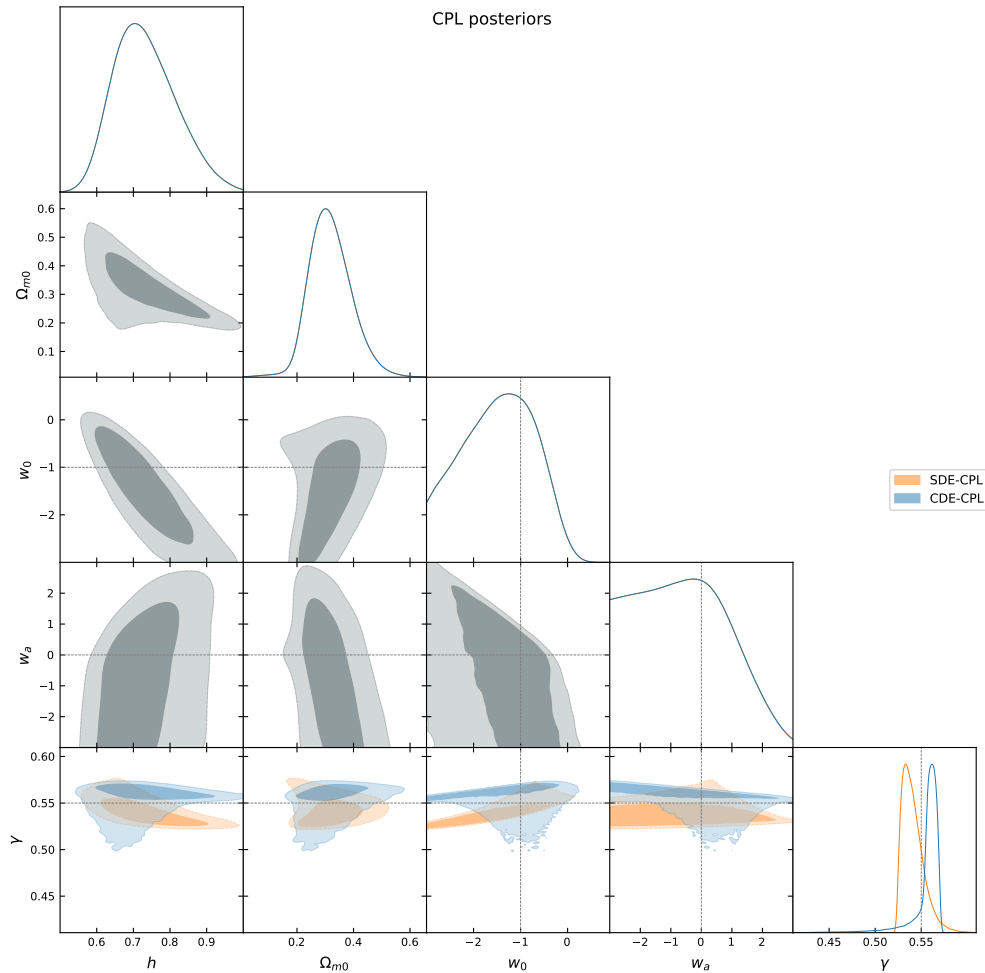


Figure 4. Marginalized posterior distributions for the CPL models, with a shared background and distinct Smooth and Clustering Dark Energy growth index distributions. The dashed lines indicate the values of the Λ CDM parameters.

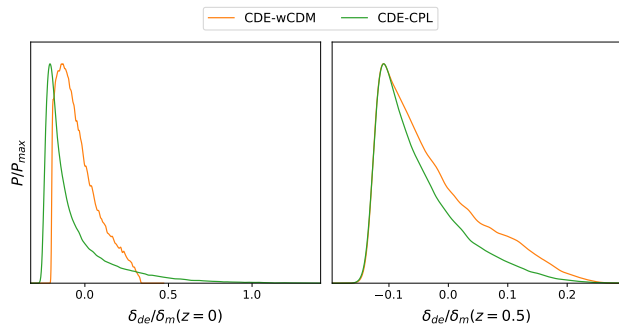


Figure 5. Distribution of perturbation ratios for w CDM and CPL models at $z = 0$ (left panel) and $z = 0.5$ (right panel).

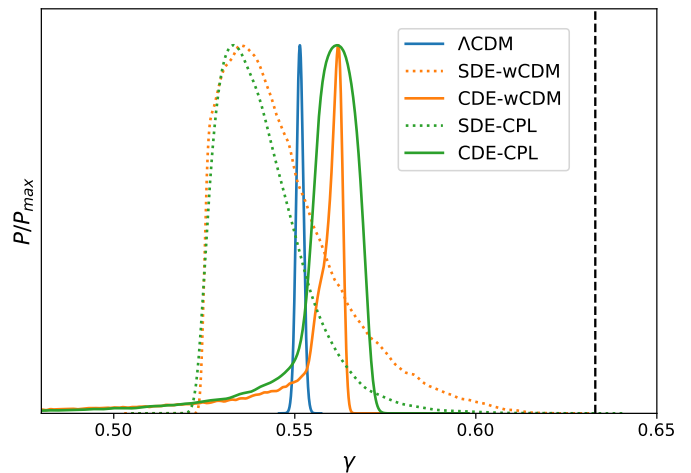


Figure 6. Distribution for γ in different models. The vertical dashed line marks the measured value $\gamma = 0.633$ for the Λ CDM background.

by the CC data. This study was helpful to analyse the accuracy of the constant γ parametrization, the possible γ values and determine more general and accurate fitting functions. Now we turn our attention to whether DE models have any significant tension with the high

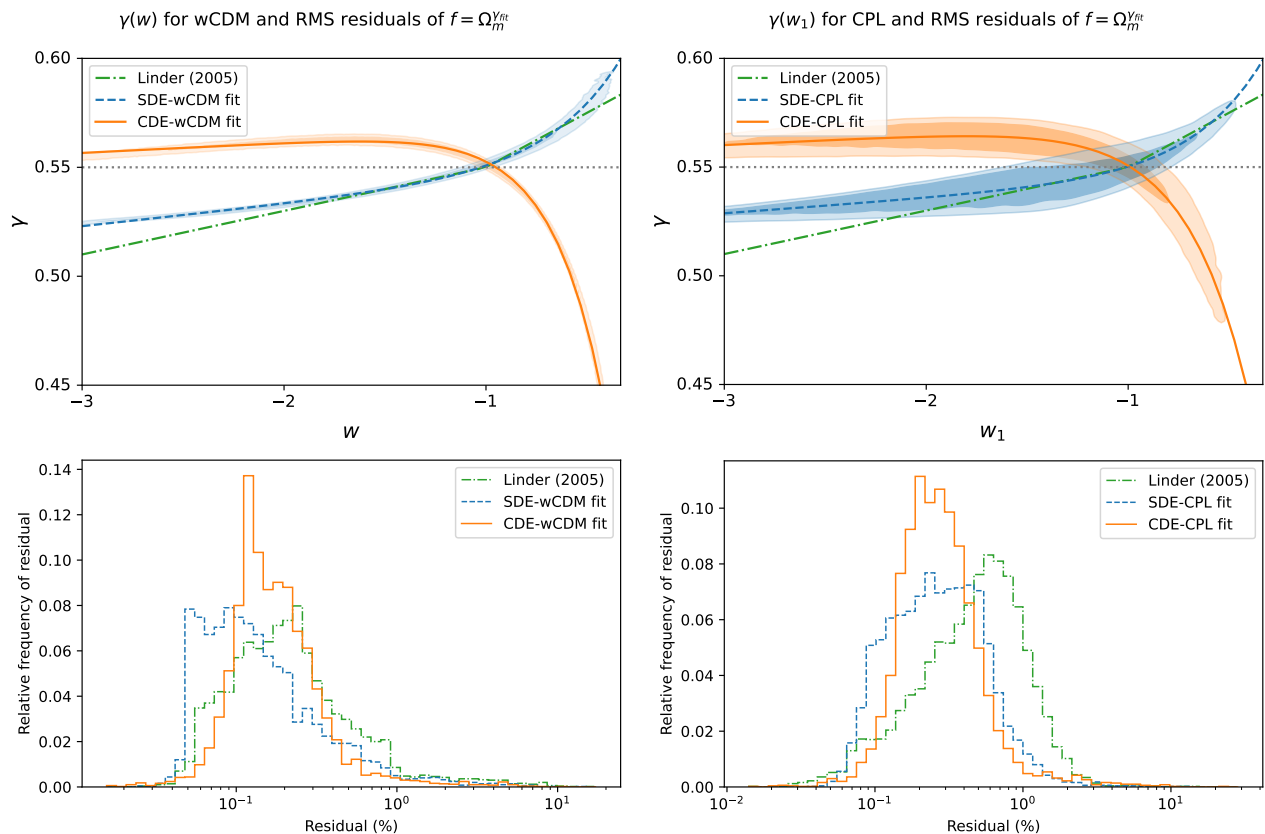


Figure 7. Different fits of $\gamma(w_1)$ for w CDM models (left panels) and for CPL models (right panels) with contours for $\gamma(w_1)$ for SDE (blue) and CDE (orange) in the upper panels. The lower panels show histograms, normalized by relative frequency, of the RMS percent residual between the γ given by fitting functions and the corresponding numerical value, obtained from the parametrization $f = \Omega_m^\gamma$.

values of γ , as suggested by measurement for Λ CDM. As shown in the previous section, both SDE and CDE can not provide a significant fraction realizations with $\gamma \simeq 0.63$. However, it is important to note this γ value was determined assuming the Λ CDM background, and a direct comparison between the measurement and possible values in other models might be inconsistent.

In order to make more precise estimates, in this section, we constrain the background parameters using DESI DR2 BAO together with CMB correlated priors on $(\theta_*, \omega_b, \omega_{bc})_{\text{CMB}}$, where $\omega_b = \Omega_{b0} h^2$ is the baryonic physical density parameter, $\omega_{bc} = (\Omega_{b0} + \Omega_{c0}) h^2$ is the sum of the previous quantity and the physical cold dark matter density parameter and θ_* is the angular scale of the CMB acoustic peaks, as discussed in Ref. [23]. We use the same set of priors indicated in [23]. For this analysis and following ones, we make use of CAMB [44, 45] to compute the BAO observables and the Cobaya MCMC sampler [46, 47], which has the likelihood for DESI DR2 BAO implemented. As a convergence criteria for the chains, we assume the Gelman-Rubin statistic satisfying $R - 1 < 0.01$.

In Tab. IV, we show the marginalized (68% C.L.) constraints on the background parameters and the resulting

theoretical values for γ . As can be seen, all parameters now have much smaller uncertainties with respect to the analysis using CC data, shown in the previous section, Tab. II.

To make a fast estimation of the γ values and its uncertainty in w CDM and CPL backgrounds, we proceed as follows. Assuming fiducial parameters $\Omega_{m0} = 0.3$, which is the visualized central value of the most precise measurement in Ref. [1] for Λ CDM, we generate a synthetic growth rate function based on the measured γ ,

$$f_{\text{syn}}(z) = \Omega_{m\Lambda}^{0.633}(z). \quad (18)$$

We use this function to generate 18 mock data points of $f_{\text{syn}}(z)$, evenly spaced in the range $0 \leq z \leq 0.9$ with normally distributed 7% scatter around the fiducial values. Then we use the mock data points in an uncorrelated Gaussian likelihood function for $f_{\text{syn}}(z)$.

With this setup, realizations of $f_{\text{syn}}(z)$ with 7% uncertainty converge to reproduce the measured constraints on γ obtained in Ref. [1]. We choose a particular realization that yields constraints shown in the middle section of Tab. IV, in particular, $\gamma = 0.625 \pm 0.023$ for Λ CDM. Note that, as stated in the DESI BAO DR2 analysis, Ref. [23],

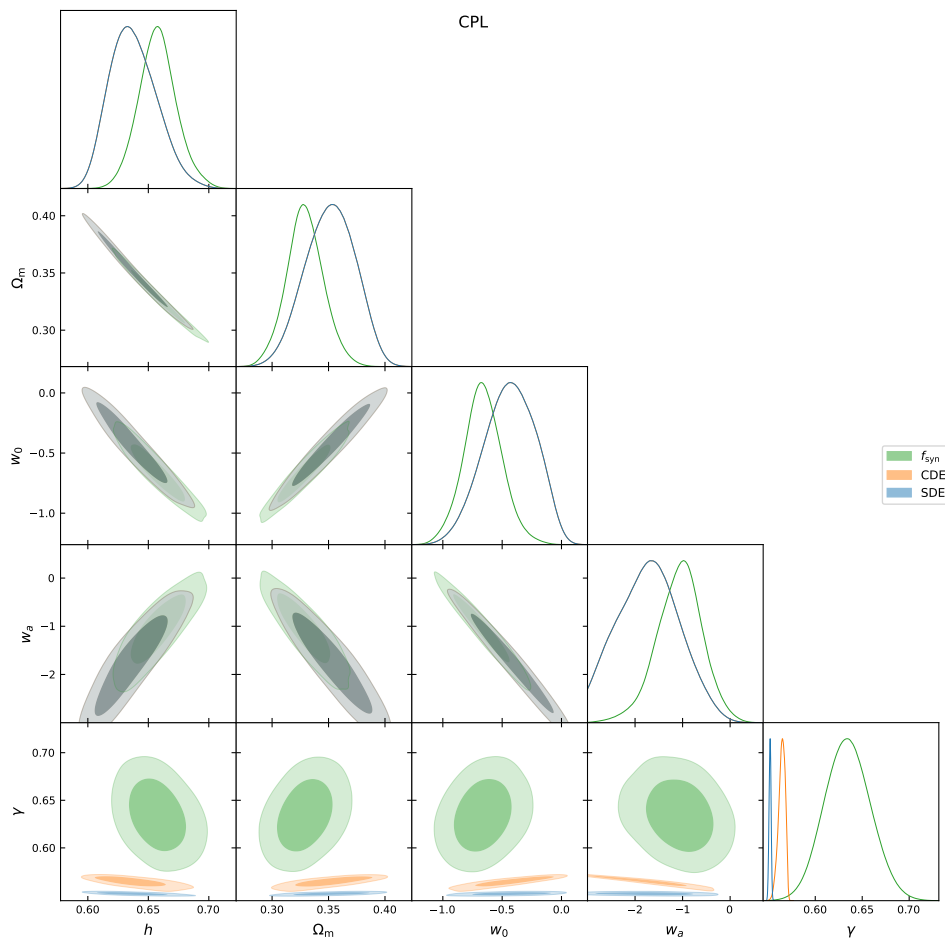


Figure 8. Marginalized posterior distributions for the CPL background: constrained by DESI BAO DR2 + $(\theta_*, \omega_b, \omega_{bc})_{\text{CMB}}$ and corresponding theoretical γ values for SDE and CDE models and the estimated constraints on γ (f_{syn}) using DESI BAO DR2 + $(\theta_*, \omega_b, \omega_{bc})_{\text{CMB}}$ + f_{syn} data. Note that SDE and CDE models share the same distributions for background parameters.

these measurements are based on a dataset that is essentially background-dependent and model-independent.

For w CDM, as can be seen in Tab. IV and in Fig. 9, the central value of the estimated γ is very close to the measured one for Λ CDM. For CPL, there is a small increase in the estimated γ , shown in Tab. IV and in Fig. 10. In both cases, the uncertainty in γ is close to the one found for Λ CDM. This finding is somewhat unexpected because usually measurements for models with larger parameter space are more inaccurate. We checked that this actually occurs when using Gaussian uncorrelated priors based on the posteriors obtained for the background parameters. Moreover, we also tested the estimation of γ constraining the background with CC data. In this case, given the much larger allowed parameter space volume, we also see a relevant increase in the γ uncertainty for w CDM and CPL models. Finally, we checked that less precise mock data, yielding 0.028 uncertainty for γ in Λ CDM model, support the same conclusions of nearly unchanged γ central values and uncertainties for the other backgrounds when using DESI BAO DR2

+ $(\theta_*, \omega_b, \omega_{bc})_{\text{CMB}}$. Therefore, we understand that the same level of uncertainty for γ for all backgrounds is due to the high constraining power and strong correlations in the background parameters determined by DESI BAO DR + $(\theta_*, \omega_b, \omega_{bc})_{\text{CMB}}$.

As a visual example of these correlations, some of which were already shown in Ref. [23], in Fig. 8, we show the posteriors for the CPL model parameters. We can also see that the inclusion of f_{syn} data has some impact on the central value of background parameters and decreases their uncertainties. In particular, the determination of w_a has a relevant improvement in its determination, excluding the lowest values permitted by the background analysis. In this figure, note that SDE and CDE have the same background posteriors.

In Figs. 9 and 10, we show the theoretical predictions for γ in w CDM and CPL models and γ estimated measurements. As can be seen, for w CDM, the central value is basically the same for SDE and CDE. This is expected because the posterior of w gives $w \simeq -1$ with small uncertainties, making CDE effects much smaller than those

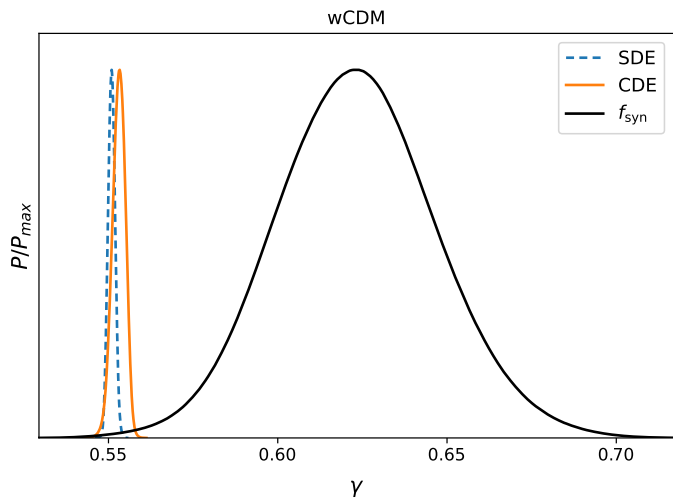


Figure 9. Distribution for γ in w CDM model for SDE and CDE and the estimated constraints on γ based on f_{syn} data with 7% uncertainty.

seen in Fig. 6. In the CPL case, we see a more significant difference between the central γ values for SDE and CDE, with the latter giving higher values. As explained earlier, this is a manifestation of the preference for phantom EoS (at least for some period of the cosmic expansion), which is favored by DESI data, mainly due to preference for negative w_a .

In the present analysis, the theoretical γ distributions are much less asymmetric than the more general distributions shown in Sect. IV. Therefore, we can more safely estimate the level of tension, as defined in Eq. (16) for Gaussian distributions. These results are shown in the bottom section of Tab. IV. For the CDE cases, which still have slightly asymmetric 1σ limits, we use the larger value. As can be seen, the tension is similar in all models, except for smooth CPL, which has a slightly increased tension with the estimated γ . This occurs because the central value of Ω_{m0} for the CPL background has a significant increase with respect to the Λ CDM or w CDM values. As a consequence, in order to have a similar growth rate, γ has to increase. Since the smooth CPL model has a very limited variation of γ , around the Λ CDM value, the tension increases. On the other hand, given the perturbative behavior already explained, the clustering CPL model has more freedom to raise the γ value, resulting in a lower tension with respect to its smooth counterpart.

Therefore, also when constraining the background parameters with $\text{DESI}+(\theta_*, \omega_b, \omega_{bc})_{\text{CMB}}$, neither SDE nor CDE with CPL EoS can raise the mode of their γ distributions to high values, $\gamma > 0.6$. Moreover, our method to estimate γ for w CDM and CPL backgrounds does not indicate any significant variation of it with respect to the measured value for the Λ CDM model and quite similar uncertainties, which is likely caused by the highly constrained background parameters and their strong correlations.

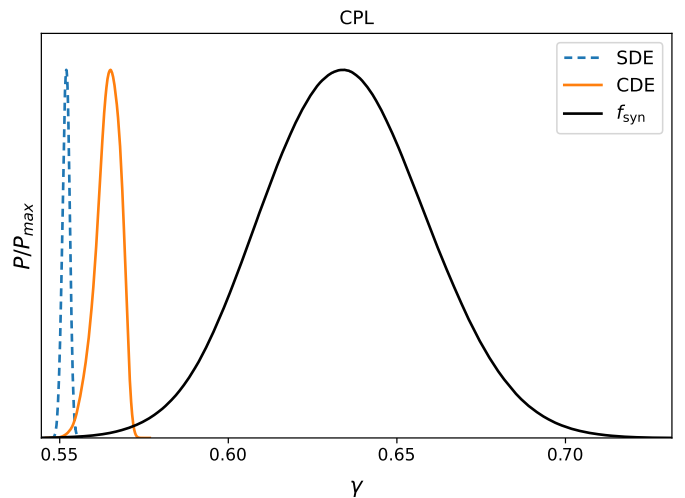


Figure 10. Distribution for γ in CPL model for theoretical SDE and CDE models and estimated constraints of γ based on f_{syn} data with 7% uncertainty.

If future analysis confirm this high value for w CDM and CPL backgrounds, DE models will be challenged. Furthermore, it is interesting to highlight that, given that CPL background subjected to $\text{DESI}+(\theta_*, \omega_b, \omega_{bc})_{\text{CMB}}$ data has higher Ω_{m0} , which enhances the growth rate, there is a natural tendency for higher γ , which counteracts this enhancement. Thus, it is quite likely that γ tension can not be alleviated by smooth CPL models. However, the concrete tension level crucially depends on γ measurements with real data.

VI. CONCLUSIONS

In this paper, we have analyzed the possibilities of DE models described by the CPL parametrization of producing a high γ values, in line with $\gamma = 0.633$ obtained in Ref. [1] for Λ CDM. As summarized in Fig. 6, both smooth DE and clustering DE have γ distributions with central values below 0.56. This result depends only on the following assumptions: (1) $H(z)$ must be compatible with CC data, (2) $\Omega_{de}(z=1000) < 0.01$ and (3) the priors described in Tab. I. The combination of these assumptions imposes very loose constraints on $w_0 w_a$ parameters, allowing for a vast, but meaningful, exploration of the possible values of γ .

We analyzed the correlations between γ , the EoS parameters and the clustering properties of DE. In particular, we can expect that phantom CDE models can raise the value of γ . However, since the impact of such models depend on $\Omega_{de}(z)\delta_{de}(z)$, the actual change is very limited because $\Omega_{de}(z)$ decays rapidly with z . Non-phantom SDE can also give higher γ , but these realizations are correlated with very low matter density parameter, $\Omega_{m0} \simeq 0.1$.

We also proposed a new fitting function for $\gamma = \gamma(w_1)$,

Table IV. Upper section: marginalized (68% C.L.) constraints on the background parameters using DESI + $(\theta_*, \omega_b, \omega_{bc})_{\text{CMB}}$ data and the resulting theoretical γ constraints. Middle section: marginalized (68% C.L.) constraints on parameters using DESI + $(\theta_*, \omega_b, \omega_{bc})_{\text{CMB}} + f_{\text{syn}}$ data and the corresponding estimated γ constraints for each background. Bottom section: tension between the theoretical and estimated γ values.

Dataset/Parameter	ΛCDM	$w\text{CDM}$	CPL
DESI-DR2 + $(\theta_*, \omega_b, \omega_{bc})_{\text{CMB}}$			
h	$0.6836^{+0.0028}_{-0.0031}$	0.6904 ± 0.0097	$0.638^{+0.017}_{-0.022}$
Ω_{m0}	0.3005 ± 0.0038	0.2957 ± 0.0076	0.351 ± 0.022
w or w_0	---	-1.029 ± 0.039	-0.44 ± 0.22
w_a	---	---	-1.67 ± 0.64
γ (SDE)	$0.551678^{+0.000059}_{-0.000070}$	0.5509 ± 0.0010	0.5519 ± 0.0011
γ (CDE)	---	$0.5530^{+0.0021}_{-0.0017}$	$0.5644^{+0.0043}_{-0.0028}$
DESI-DR2 + $(\theta_*, \omega_b, \omega_{bc})_{\text{CMB}} + f_{\text{syn}}$			
h	0.6834 ± 0.0029	$0.6853^{+0.0082}_{-0.0092}$	0.647 ± 0.011
Ω_{m0}	0.3008 ± 0.0038	0.2994 ± 0.0070	0.340 ± 0.012
w or w_0	---	$-1.008^{+0.037}_{-0.033}$	-0.54 ± 0.12
w_a	---	---	-1.41 ± 0.36
γ (f_{syn})	0.625 ± 0.023	0.624 ± 0.024	0.639 ± 0.024
Tension			
$\#\sigma$ (f_{syn} - SDE)	3.06	3.04	3.63
$\#\sigma$ (f_{syn} - CDE)	---	2.95	3.06

with overall accuracies better than the linear fit of Eq. (3) covering the interval of $-3 \leq w_1 \leq -1/3$. For the first time, we produced a γ fitting function for CDE models, Eq. (17) with coefficients given in Tab. III. These fits can be useful for a fast determination of γ for both SDE and CDE models described by CPL parametrization.

In a more specific analysis, we have computed the theoretical γ distributions constraining the background parameters using DESI BAO DR2 + $(\theta_*, \omega_b, \omega_{bc})_{\text{CMB}}$ data. Also in this case, the γ values are not allowed to reach high values, obtaining central values with $\gamma \lesssim 0.57$. In the same context for background constraints, we also estimated the γ values for $w\text{CDM}$ and CPL models based on mock data generated for the growth rate function. This analysis indicated no significant change in the estimated γ distribution and its uncertainty with respect to the measured value for ΛCDM . Consequently, this preliminary study suggests that the DE models considered in this work can have roughly the same level of γ tension as found for ΛCDM , with a small tension decrease for CDE models relative to the SDE ones.

If the high γ value found in Ref. [1] is validated by other observations and analysis [48] and for backgrounds beyond ΛCDM , it poses a significant challenge to DE

models based on minimally coupled scalar fields that can be described by the CPL EoS and a constant c_s on small scales because these models are incapable to provide such high γ values. Since we have considered the two limiting cases of smooth DE ($c_s = 1$) and full clustering DE ($c_s = 0$), it seems unlikely that intermediate or time-varying c_s values can produce a significantly higher γ . A possible alternative is to consider more general EoS parametrizations. However, as demonstrated in our study, large variations on the EoS parameters and Ω_{m0} produce much narrower γ distributions. Therefore, in principle, even more general EoS parametrizations should have some difficulties in explaining such high γ values, with the disadvantage of introducing more parameters. If this ‘ γ tension’ persists, we might be seeing an early evidence of modified gravity or non-standard dark matter.

ACKNOWLEDGMENTS

We thank Valerio Marra for useful discussions. IBSC thanks Universidade Federal do Rio Grande do Norte for the undergraduate research scholarship, N^o 01/2023 (PIBIC-PROPESQ) project PIJ20915-2023.

[1] N.-M. Nguyen, D. Huterer, and Y. Wen, Evidence for Suppression of Structure Growth in the Concordance Cosmological Model, Phys. Rev. Lett. **131**, 111001 (2023), arXiv:2302.01331 [astro-ph.CO].

[2] E. V. Linder, Cosmic growth history and expansion history, Phys. Rev. **D72**, 043529 (2005), astro-ph/0507263.

[3] E. Abdalla *et al.*, Cosmology intertwined: A review of the particle physics, astrophysics, and cosmology associated

- with the cosmological tensions and anomalies, *JHEAp* **34**, 49 (2022), arXiv:2203.06142 [astro-ph.CO].
- [4] A. G. Riess, W. Yuan, L. M. Macri, D. Scolnic, D. Brout, S. Casertano, D. O. Jones, Y. Murakami, L. Breuval, T. G. Brink, A. V. Filippenko, S. Hoffmann, S. W. Jha, W. D. Kenworthy, G. Anand, J. Mackenty, B. E. Stahl, and W. Zheng, A comprehensive measurement of the local value of the hubble constant with 1 km/s/mpc uncertainty from the hubble space telescope and the sh0es team, *The Astrophysical Journal Letters* **934**, L7 (2021), arXiv:2112.04510 [astro-ph.CO].
- [5] N. Aghanim *et al.* (Planck), Planck 2018 results. vi. cosmological parameters, *Astron. Astrophys.* **641**, A6 (2020), [Erratum: *Astron. Astrophys.* 652, C4 (2021)], arXiv:1807.06209 [astro-ph.CO].
- [6] E. Di Valentino *et al.*, Cosmology intertwined iii: $f\sigma_8$ and s_8 , *Astropart. Phys.* **131**, 102604 (2021), arXiv:2008.11285 [astro-ph.CO].
- [7] R. C. Nunes and S. Vagnozzi, Arbitrating the S8 discrepancy with growth rate measurements from redshift-space distortions, *Mon. Not. Roy. Astron. Soc.* **505**, 5427 (2021), arXiv:2106.01208 [astro-ph.CO].
- [8] S. A. Adil, O. Akarsu, M. Malekjani, E. O. Colgáin, S. Pourojaghi, A. A. Sen, and M. M. Sheikh-Jabbari, S8 increases with effective redshift in Λ CDM cosmology, *Mon. Not. Roy. Astron. Soc.* **528**, L20 (2023), arXiv:2303.06928 [astro-ph.CO].
- [9] M. S. Madhavacheril *et al.* (ACT), The Atacama Cosmology Telescope: DR6 Gravitational Lensing Map and Cosmological Parameters, *Astrophys. J.* **962**, 113 (2024), arXiv:2304.05203 [astro-ph.CO].
- [10] L. Amendola *et al.* (Euclid Theory Working Group), Cosmology and fundamental physics with the Euclid satellite, *Living Rev. Rel.* **16**, 6 (2013), arXiv:1206.1225 [astro-ph.CO].
- [11] L.-M. Wang and P. J. Steinhardt, Cluster abundance constraints on quintessence models, *Astrophys. J.* **508**, 483 (1998), astro-ph/9804015.
- [12] P. J. E. Peebles and B. Ratra, Cosmology with a time variable cosmological 'constant', *Astrophys. J.* **325**, L17 (1988).
- [13] B. Ratra and P. J. E. Peebles, Cosmological consequences of a rolling homogeneous scalar field, *Phys. Rev.* **D37**, 3406 (1988).
- [14] C. Wetterich, Cosmology and the fate of dilatation symmetry, *Nucl. Phys.* **B302**, 668 (1988).
- [15] R. C. Batista, H. P. de Oliveira, and L. R. W. Abramo, Spherical collapse of non-top-hat profiles in the presence of dark energy with arbitrary sound speed, *JCAP* **02**, 037, arXiv:2210.14769 [astro-ph.CO].
- [16] C. Armendariz-Picon, T. Damour, and V. F. Mukhanov, k - inflation, *Phys. Lett. B* **458**, 209 (1999), arXiv:hep-th/9904075.
- [17] C. Armendariz-Picon, V. F. Mukhanov, and P. J. Steinhardt, Essentials of k -essence, *Phys. Rev.* **D63**, 103510 (2001), arXiv:astro-ph/0006373.
- [18] R. C. Batista, A Short Review on Clustering Dark Energy, *Universe* **8**, 22 (2021), arXiv:2204.12341 [astro-ph.CO].
- [19] R. C. Batista, Impact of dark energy perturbations on the growth index, *Phys. Rev.* **D89**, 123508 (2014), arXiv:1403.2985 [astro-ph.CO].
- [20] A. Mehrabi, S. Basilakos, and F. Pace, How clustering dark energy affects matter perturbations, *Mon. Not. Roy. Astron. Soc.* **452**, 2930 (2015), arXiv:1504.01262 [astro-ph.CO].
- [21] A. Mehrabi, S. Basilakos, M. Malekjani, and Z. Davari, Growth of matter perturbations in clustered holographic dark energy cosmologies, *Phys. Rev. D* **92**, 123513 (2015), arXiv:1510.03996 [astro-ph.CO].
- [22] A. Mehrabi, M. Malekjani, and F. Pace, Can observational growth rate data favor the clustering dark energy models?, *Astrophys. Space Sci.* **356**, 129 (2015), arXiv:1411.0780 [astro-ph.CO].
- [23] M. Abdul Karim *et al.* (DESI), DESI DR2 Results II: Measurements of Baryon Acoustic Oscillations and Cosmological Constraints, (2025), arXiv:2503.14738 [astro-ph.CO].
- [24] M. Chevallier and D. Polarski, Accelerating universes with scaling dark matter, *Int. J. Mod. Phys.* **D10**, 213 (2001), gr-qc/0009008.
- [25] E. V. Linder, Exploring the expansion history of the universe, *Phys. Rev. Lett.* **90**, 091301 (2003), astro-ph/0208512.
- [26] A. Favale, A. Gomez-Valent, and M. Migliaccio, Cosmic chronometers to calibrate the ladders and measure the curvature of the universe. a model-independent study, *Monthly Notices of the Royal Astronomical Society* **523**, 3406 (2023), arXiv:2301.09591 [astro-ph.CO].
- [27] D. Foreman-Mackey, D. W. Hogg, D. Lang, and J. Goodman, emcee: The mcmc hammer, *Publications of the Astronomical Society of the Pacific* **125**, 306 (2012), arXiv:1202.3665 [astro-ph.IM].
- [28] A. Lewis, GetDist: a Python package for analysing Monte Carlo samples, (2019), arXiv:1910.13970 [astro-ph.IM].
- [29] M. Moresco, A. Cimatti, R. Jimenez, L. Pozzetti, G. Zamorani, M. Bolzonella, J. Dunlop, F. Lamareille, M. Mignoli, H. Pearce, P. Rosati, D. Stern, L. Verde, E. Zucca, C. Carollo, T. Contini, J.-P. Kneib, O. L. Fevre, S. Lilly, V. Mainieri, A. Renzini, M. Scodreggio, I. Balestra, R. Gobat, R. McLure, S. Bardelli, A. Bongiorno, K. Caputi, O. Cucciati, S. de la Torre, L. de Ravel, P. Franzetti, B. Garilli, A. Iovino, P. Kampczyk, C. Knobel, K. Kovac, J.-F. L. Borgne, V. L. Brun, C. Maier, R. Pello, Y. Peng, E. Perez-Montero, V. Presotto, J. Silverman, M. Tanaka, L. Tasca, L. Tresse, D. Vergani, O. Almaini, L. Barnes, R. Bordoloi, E. Bradshaw, A. Cappi, R. Chuter, M. Cirasuolo, G. Coppa, C. Diener, S. Foucaud, W. Hartley, M. Kamionkowski, A. Koekemoer, C. Lopez-Sanjuan, H. McCracken, P. Nair, P. Oesch, A. Stanford, and N. Welikala, Improved constraints on the expansion rate of the universe up to $z = 1.1$ from the spectroscopic evolution of cosmic chronometers, *Journal of Cosmology and Astroparticle Physics* **2012** (08), 006.
- [30] M. Moresco, Raising the bar: new constraints on the hubble parameter with cosmic chronometers at $z = 2$, *Monthly Notices of the Royal Astronomical Society: Letters* **450**, L16 (2015).
- [31] M. Moresco, L. Pozzetti, A. Cimatti, R. Jimenez, C. Maraston, L. Verde, D. Thomas, A. Citro, R. Tojeiro, and D. Wilkinson, A 6 measurement of the hubble parameter at $z = 0.45$: direct evidence of the epoch of cosmic re-acceleration, *Journal of Cosmology and Astroparticle Physics* **2016** (05), 014.
- [32] C. Zhang, H. Zhang, S. Yuan, S. Liu, T.-J. Zhang, and Y.-C. Sun, Four new observational $h(z)$ data from luminous red galaxies in the sloan digital sky survey data

- release seven, *Research in Astronomy and Astrophysics* **14**, 1221 (2014).
- [33] R. Jimenez, L. Verde, T. Treu, and D. Stern, Constraints on the equation of state of dark energy and the hubble constant from stellar ages and the cosmic microwave background, *The Astrophysical Journal* **593**, 622 (2003).
- [34] J. Simon, L. Verde, and R. Jimenez, Constraints on the redshift dependence of the dark energy potential, *Physical Review D* **71**, 123001 (2005).
- [35] A. L. Ratsimbazafy, S. I. Loubser, S. M. Crawford, C. M. Cress, B. A. Bassett, R. C. Nichol, and P. Vaisanen, Age-dating luminous red galaxies observed with the southern african large telescope, *Monthly Notices of the Royal Astronomical Society* **467**, 3239 (2017).
- [36] D. Stern, R. Jimenez, L. Verde, M. Kamionkowski, and S. A. Stanford, Cosmic chronometers: constraining the equation of state of dark energy. i: $H(z)$ measurements, *Journal of Cosmology and Astroparticle Physics* **2010** (02), 008.
- [37] N. Borghi, M. Moresco, and A. Cimatti, Toward a better understanding of cosmic chronometers: A new measurement of $h(z)$ at $z = 0.7$, *The Astrophysical Journal Letters* **928**, L4 (2022).
- [38] D. Huterer and E. V. Linder, Separating dark physics from physical darkness: Minimalist modified gravity vs. dark energy, *Phys.Rev.D75:023519,2007* **75**, 023519 (2006), arXiv:astro-ph/0608681 [astro-ph].
- [39] A. Gómez-Valent, Z. Zheng, L. Amendola, V. Pettorino, and C. Wetterich, Early dark energy in the pre- and postrecombination epochs, *Phys. Rev. D* **104**, 083536 (2021), arXiv:2107.11065 [astro-ph.CO].
- [40] L. Abramo, R. Batista, L. Liberato, and R. Rosenfeld, Physical approximations for the nonlinear evolution of perturbations in inhomogeneous dark energy scenarios, *Phys.Rev.* **D79**, 023516 (2009), arXiv:0806.3461 [astro-ph].
- [41] D. Sapone, M. Kunz, and M. Kunz, Fingerprinting dark energy, *Phys. Rev.* **D80**, 083519 (2009), arXiv:0909.0007 [astro-ph.CO].
- [42] P. Creminelli, G. D’Amico, J. Norena, and F. Vernizzi, The effective theory of quintessence: the $w < -1$ side unveiled, *JCAP* **0902**, 018, arXiv:0811.0827 [astro-ph].
- [43] R. Batista and F. Pace, Structure formation in inhomogeneous Early Dark Energy models, *JCAP* **1306**, 044, arXiv:1303.0414 [astro-ph.CO].
- [44] A. Lewis, A. Challinor, and A. Lasenby, Efficient computation of cmb anisotropies in closed frw models, *Astrophys. J.* **538**, 473 (2000), arXiv:astro-ph/9911177.
- [45] C. Howlett, A. Lewis, A. Hall, and A. Challinor, CMB power spectrum parameter degeneracies in the era of precision cosmology, *JCAP* **1204**, 027, arXiv:1201.3654 [astro-ph.CO].
- [46] J. Torrado and A. Lewis, Cobaya: Code for bayesian analysis of hierarchical physical models 10.48550/ARXIV.2005.05290 (2020).
- [47] A. Lewis and S. Bridle, Cosmological parameters from CMB and other data: A Monte Carlo approach, *Phys. Rev.* **D66**, 103511 (2002), arXiv:astro-ph/0205436 [astro-ph].
- [48] A few days after the first version of this paper was posted on arxiv.org, Ref. [49] claimed that the use of more recent likelihoods for Planck data provide γ measurements compatible with Λ CDM.
- [49] E. Specogna, W. Giarè, and E. Di Valentino, Planck-PR4 anisotropy spectra show (better) consistency with General Relativity, (2024), arXiv:2411.03896 [astro-ph.CO].